

## GaN-based blue laser diodes

This article has been downloaded from IOPscience. Please scroll down to see the full text article.

2001 J. Phys.: Condens. Matter 13 7099

(<http://iopscience.iop.org/0953-8984/13/32/315>)

View [the table of contents for this issue](#), or go to the [journal homepage](#) for more

Download details:

IP Address: 171.66.16.226

The article was downloaded on 16/05/2010 at 14:06

Please note that [terms and conditions apply](#).

## GaN-based blue laser diodes

**Takao Miyajima<sup>1</sup>, Tsuyoshi Tojyo<sup>2</sup>, Takeharu Asano<sup>2</sup>,  
Katsunori Yanashima<sup>1</sup>, Satoru Kijima<sup>2</sup>, Tomonori Hino<sup>2</sup>,  
Motonobu Takeya<sup>2</sup>, Shiro Uchida<sup>2</sup>, Shigetaka Tomiya<sup>3</sup>,  
Kenji Funato<sup>1</sup>, Tsunenori Asatsuma<sup>1</sup>, Toshimasa Kobayashi<sup>1</sup> and  
Masao Ikeda<sup>2</sup>**

<sup>1</sup> CT Development Centre, CNC, Sony Corporation, 4-14-1 Asahi-cho, Atsugi,  
Kanagawa 243-0014, Japan

<sup>2</sup> Sony Shiroishi Semiconductor Inc., 3-53-2 Shiratori, Shiroishi, Miyagi 989-0734, Japan

<sup>3</sup> Environment and Analysis Technology Department, Sony Corporation, 2-1-1  
Shin-sakuragaoka, Hodogaya, Yokohama 240-0036, Japan

Received 7 June 2001

Published 26 July 2001

Online at [stacks.iop.org/JPhysCM/13/7099](http://stacks.iop.org/JPhysCM/13/7099)

### Abstract

We report our recent progress on GaN-based high-power laser diodes (LDs), which will be applied as a light source in high-density optical storage systems. We have developed raised-pressure metal–organic chemical vapour deposition (RP-MOCVD), which can reduce the threading-dislocation density in the GaN layer to several times  $10^8 \text{ cm}^{-2}$ , and demonstrated continuous-wave (cw) operation of GaN-based LD grown by RP-MOCVD. Furthermore, we found that the epitaxial lateral overgrowth (ELO) technique is useful for further reducing threading-dislocation density to  $10^6 \text{ cm}^{-2}$  and reducing the roughness of the cleaved facet. By using this growth technique and optimizing device parameters, the lifetime of LDs was improved to more than 1000 hours under 30 mW cw operation at 60 °C. Our results proved that reducing both threading-dislocation density and consumption power is a valid approach to realizing a practical GaN-based LD. On the other hand, the practical GaN-based LD was obtained when threading-dislocation density in ELO-GaN was only reduced to  $10^6 \text{ cm}^{-2}$ , which is a relatively small reduction as compared with threading-dislocation density in GaAs- and InP-based LDs. We believe that the multiplication of non-radiative centres is very slow in GaN-based LDs, possibly due to the innate character of the GaN-based semiconductor itself.

### 1. Introduction

GaN-based semiconductors have been studied as a promising material for the light source of high-density optical storage system. After Akasaki *et al* [1] reported current-injected stimulated emission in 1995 and Nakamura *et al* reported room-temperature pulsed [2] and

continuous-wave (cw) lasing operation [3] of GaN-based blue laser diode (LD) in 1996, respectively, many research groups achieved cw operation [4–13]. Recently, Nichia [14] and Sony [15] achieved the practical long lifetime of more than 1000 hours under a high optical output power of 30 mW. Then, several groups [16, 17] demonstrated an optical storage system with a capacity of over 22 GB using a GaN-based blue LD in 1999. These successes of GaN-based LDs are based on two novel growth techniques for reducing threading-dislocation density. The first technique is low-temperature buffer [18, 19], and the second technique is epitaxial lateral overgrowth (ELO) [20, 21].

For lack of a large GaN substrate, a GaN-based semiconductor is grown on a sapphire or a SiC substrate which is stable in ammonia atmosphere at a high growth temperature of around 1000 °C. However, the heteroepitaxy generates a high density of threading dislocation (more than  $10^{11}$  cm<sup>-2</sup>) and cracks in the GaN layer grown on the substrate because of the large lattice mismatch and difference between the thermal-expansion coefficients of GaN and these substrate materials. After the low-temperature buffer [18, 19] was developed, the threading-dislocation density could be reduced below  $10^{10}$  cm<sup>-2</sup>. This breakthrough was essential to realize p-type GaN:Mg [22] and candela-class high-brightness GaN-based light-emitting diodes (LEDs) [23]. At the time, it was believed that the dislocations might not act as efficient non-radiative recombination centres because there were still many threading dislocations of  $10^{10}$  cm<sup>-2</sup> in the device [24, 25]. On the other hand, a lifetime of more than 10 000 hours under an output power of 2 mW was achieved by Nakamura *et al* [26] using the ELO technique, which was originally developed as a method of reducing threading-dislocation density by Nishinaga *et al* in 1988 [27], and applied to GaN-based semiconductors by Usui *et al* [20] and Nam *et al* [21] in 1997. It would seem that a high dislocation density limits the lifetime of GaN-based LDs and must be reduced to realize a practical device.

Most research groups use a ridge-type structure for a GaN-based LD [3–13]. This simple structure is suitable for mass-production, but has a disadvantage in that the distribution of current and light parallel (lateral) to the junction plane cannot be controlled separately. To address this problem, we investigated the feasibility of a GaN-based LD with a buried-ridge structure. After demonstrating cw operation [28], we found that the optical transverse mode in the LD can be controlled by adjusting the Al content of the Al<sub>x</sub>Ga<sub>1-x</sub>N buried layer and the characteristics of the LD could also be changed from gain guiding to index guiding [28–30].

In this paper, we describe how dislocation density can be reduced and report our recent progress on GaN-based high-power LDs.

## 2. Properties of threading dislocations in GaN

Threading-dislocation density is an important parameter for evaluating the GaN-layer's quality and is generally measured using a plan-view transmission electron microscopy (TEM) and etch-pit density (EPD) observation. For TEM observation, however, sample preparation is very complicated and it is difficult to observe a low density of threading dislocations below  $1 \times 10^6$  cm<sup>-2</sup>. EPD observation is a simple method and the observed area only depends on the sample size, but there is no suitable chemical solvent to selectively etch all different species of threading dislocations [31, 32]. We have developed a new simple method to observe etch pits after HCl vapour phase etching [33]. Using this technique, we can categorize the threading dislocations in the GaN layer into three types of line defect: edge, screw and mixed dislocation and individually measure the density.

We next investigated the effect of threading dislocations on the optical properties of GaN by measuring the EPD, photoluminescence (PL) intensity and decay time of n-type GaN:Si. As shown in figures 1 and 2, the room-temperature PL intensity and decay time decreases with

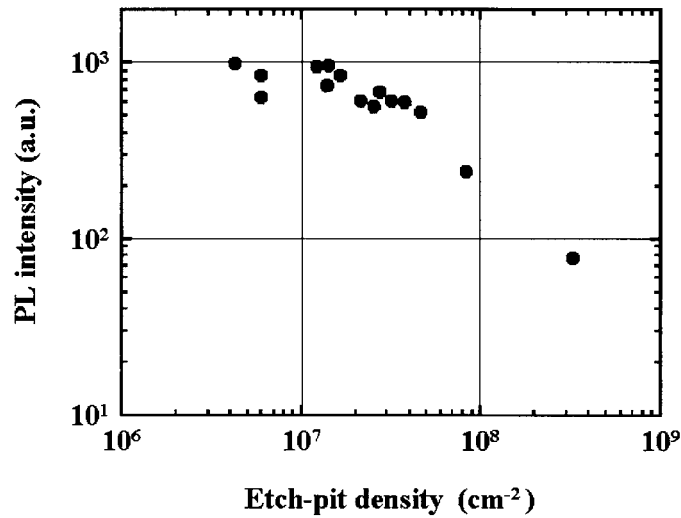


**Figure 1.** Dependence of room-temperature PL intensity on EPD, which corresponds to the total density of screw and mixed dislocations in n-type GaN:Si [33].

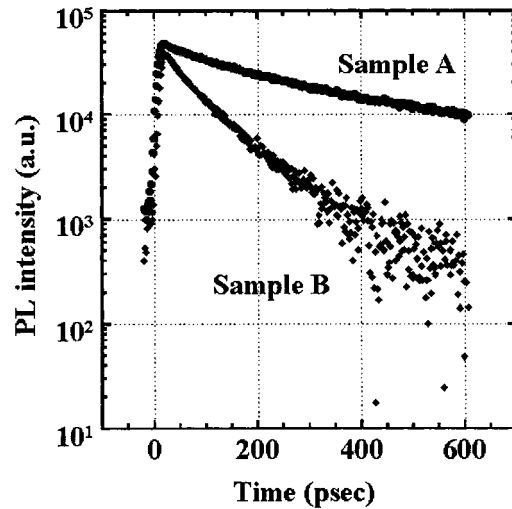


**Figure 2.** Time-resolved PL spectrum at room temperature for GaN:Si [34]. Samples A and B have a total density of screw and mixed dislocations of  $3.7 \times 10^6 \text{ cm}^{-2}$  and  $3.2 \times 10^8 \text{ cm}^{-2}$ , respectively.

the increase of the total density of screw and mixed dislocations while Si of  $2 \times 10^{18} \text{ cm}^{-3}$  was constantly doped to the GaN layer as the radiative centre. These dependences suggest that screw and mixed dislocations, which have screw-component Burgers vectors, strongly influence the radiative efficiency and act as strong non-radiative centres in the GaN epitaxial layer. We have confirmed that the other line defect, edge dislocation, also acts as a non-radiative centre [34] and have therefore concluded that the density of all line defects must be reduced to realize a high-optical-quality GaN layer and GaN-based laser diodes. It remained to be determined, however, to what extent threading dislocations would have to be reduced in order to realize GaN-based laser diode with a practical lifetime.

### 3. Raised-pressure metal–organic chemical vapour deposition

#### 3.1. Reduction of threading dislocation density

We had considered that the way to realize a high-performance GaN-based laser diode was to improve the crystalline quality of a GaN-based semiconductor grown on a sapphire substrate. We thought however that because of the high dissociation pressure of GaN, it would be very difficult to grow high-quality GaN using metal–organic chemical vapour deposition (MOCVD). We have solved this problem by growing GaN layers under nitrogen overpressure during growth in order to minimize the density of non-radiative centres. We call this growth method raised-pressure metal–organic chemical vapour deposition (RP-MOCVD). The detailed growth conditions have been reported elsewhere [35].

First, we investigated the crystalline quality of GaN:Si grown on sapphire by RP-MOCVD using optical pumping measurements. A 30 nm thick GaN buffer layer was first grown on a sapphire substrate, followed by a 1  $\mu\text{m}$  thick undoped GaN layer and a 1.5  $\mu\text{m}$  thick n-type GaN:Si layer. The electron concentration of n-type GaN:Si was  $2 \times 10^{18} \text{ cm}^{-3}$ . A 2 mm long cavity with (11–20) GaN facets was prepared by cleaving the sample. Stimulated emission was observed by exciting the sample using 337 nm wavelength light of an  $\text{N}_2$  laser. As shown in figure 3, the threshold optical power density dramatically decreases as the growth pressure increases beyond 1 atm. This indicates that non-radiative centres in the GaN are significantly reduced as nitrogen overpressure increases during the growth.

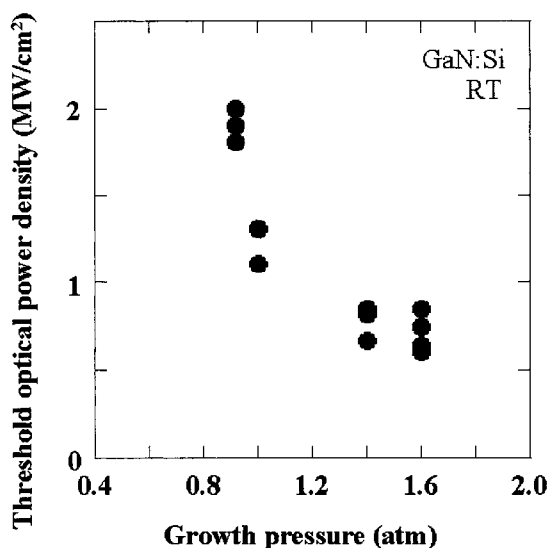


**Figure 3.** Threshold optical power density for stimulated emission as a function of growth pressure [35].

The threading-dislocation density was also measured by counting EPDs on the GaN surface after thermal HCl vapour phase etching [33]. In this experiment, screw and mixed dislocations of three types of line defect were counted because we found that the radiative efficiency of GaN:Si strongly depends on their density, as shown in figure 1. As shown in figure 4, the total density of screw and mixed dislocations decreases as growth pressure increases. This confirms that the crystalline quality was improved as growth pressure increases. The GaN layer with the highest radiative efficiency contained edge, screw and mixed dislocations of  $2 \times 10^8 \text{ cm}^{-2}$ ,

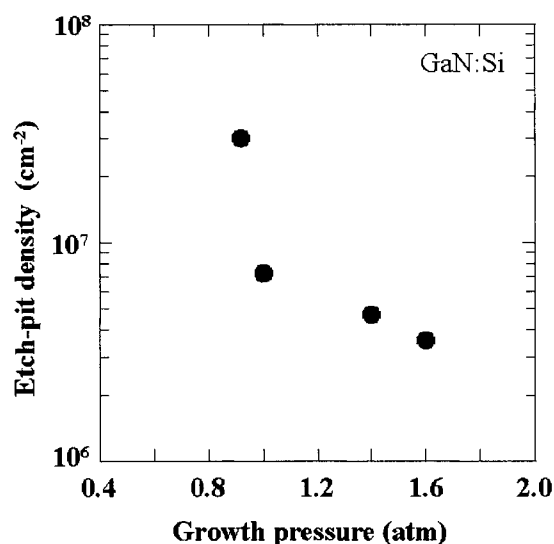


**Figure 4.** Dependence of EPD on growth pressure. EPD corresponds to the total density of screw and mixed dislocations in n-type GaN:Si [35].

$7 \times 10^5 \text{ cm}^{-2}$  and  $3 \times 10^6 \text{ cm}^{-2}$ , respectively. Typically, if the ratio of mixed dislocations to total threading dislocations is low, the GaN layer has the high radiative efficiency. We believe that the grain size of the GaN buffer layer becomes larger when the growth temperature is elevated to around  $1000^\circ\text{C}$  at 1.6 atm after the growth of the buffer layer at a lower temperature of around  $500^\circ\text{C}$ , and we believe that mixed and screw dislocations are created where the grains coalesce.

We investigated the relation between the growth pressure and the residual strain in the GaN layer. The residual strain was estimated by measuring the lattice constants of the  $c$ -axis and  $a$ -axis using x-ray diffraction. The details of this procedure are described elsewhere [36]. The lattice constants  $c$  are plotted against lattice constants  $a$  in figure 5. This figure shows a linear dependence and that the residual strain of the GaN layers grown at 1.6 atm is larger than that of layers grown at 0.9 atm. The threshold optical power density and EPD decrease as growth pressure increases. Therefore, the lesser lattice relaxation of the GaN layers grown at 1.6 atm can be attributed to the decrease in threading-dislocation density [36].

### 3.2. Improvement of LD characteristics and cw operation

The effect of RP-MOCVD on the crystalline quality was determined by observing the threshold-current density of laser diodes grown at various pressures, as shown in figure 6. The LDs were operated under a pulsed condition with a duty ratio of 0.1%. The threshold current density clearly decreases with growth pressure. We believe this is due to the higher crystalline quality of the layers grown at 1.6 atm. Moreover, the high crystalline quality was confirmed by room-temperature cw operation of laser diodes grown at 1.6 atm [35]. The threshold current was 140 mA, which corresponds to a threshold current density of  $3.5 \text{ kA cm}^{-2}$ . The operating voltage at the threshold was 16.8 V. The emission wavelength was around 405 nm. The lifetime of the device was a few seconds.

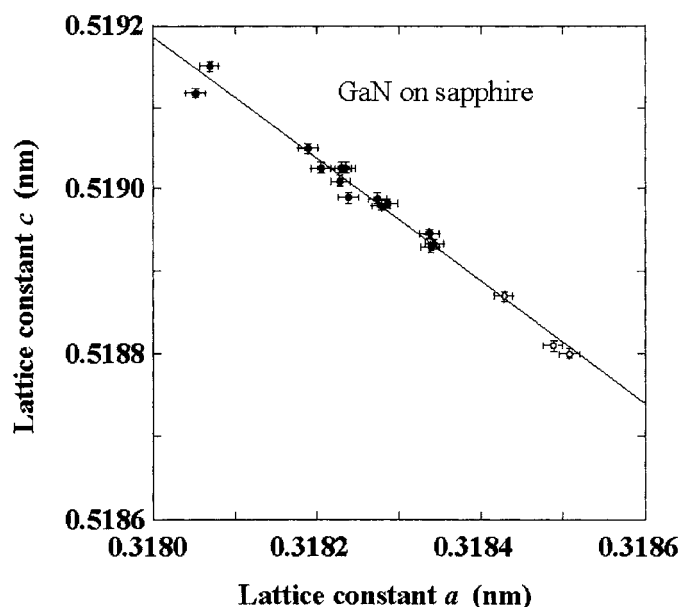


**Figure 5.** Lattice constant  $a$  against lattice constant  $c$  measured at 299 K using x-ray diffraction [36]. The open circles and closed ones correspond to samples grown under a pressure of 0.9 atm and 1.6 atm, respectively.

#### 4. Characteristics of ELO-GaN

##### 4.1. Further reduction of threading dislocation density

ELO is a novel method for further reducing threading-dislocation density below  $10^6 \text{ cm}^{-2}$  [20, 21] and so significantly improving the lifetime of GaN-based LDs [26]. However, some problems remain in obtaining an ELO-GaN layer of high structural quality. In particular, crystallographic axes are tilted in the wing region (overgrown GaN) [37–39]. The crystallographic tilt creates a tilt boundary and new dislocations at the coalescence sites. We found that the tilt strongly depends on the mask species [39–41]. On the other hand, ELO without a mask was developed by Zheleva *et al* [42] and applied to GaN-based LDs by Nakamura *et al* [43]. It was found that this growth technique is useful because the previous problem due to the mask is removed. Then we confirmed the property of ELO-GaN without a mask and applied this layer to GaN-based LDs [44, 45], as follows.

A  $2 \mu\text{m}$  thick GaN layer was grown on a  $c$ -face sapphire substrate, and silicon dioxide ( $\text{SiO}_2$ ) was deposited and patterned, forming a  $2 \mu\text{m}$  wide stripe mask with a periodicity of  $12 \mu\text{m}$  in the  $\langle 1-100 \rangle$  direction of the GaN. The GaN window region was then etched out by reactive ion etching (RIE), and the  $\text{SiO}_2$  mask was subsequently removed by wet etching. GaN was then laterally overgrown using the rectangular GaN stripes as seeds.

The PL intensity profile of the ELO-GaN was measured along a line perpendicular to the ELO stripes, as shown in figure 7. The probe wavelength was 362 nm. The PL intensity in the ELO region was found to be over three times that in the seed region, and a 30% decrease in PL intensity was found in the coalescence region. Since this PL intensity profile is related to the defect distribution, the wing region between the coalescence and seed regions should contain a low density of dislocations. This was confirmed by EPD measurements as shown in figure 8,

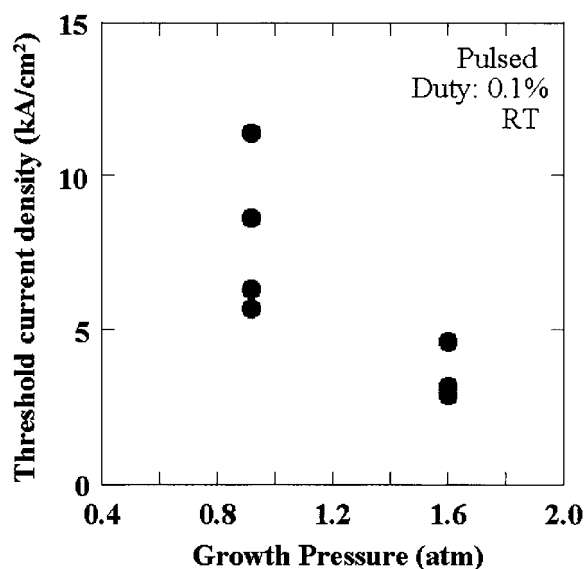


**Figure 6.** Threshold current density of laser diodes under pulsed operation with a 0.1% duty ratio as a function of growth pressure [35].

which depicts a SEM image of an etched ELO-GaN surface. In the wing region, all three types of line defect were reduced. The edge-dislocation density was  $1 \times 10^6 \text{ cm}^{-2}$ , and screw and mixed dislocation densities were less than  $10^5 \text{ cm}^{-2}$  and less than  $10^5 \text{ cm}^{-2}$  respectively, which means that no screw or mixed dislocations were detected in the observed area. The same density of threading dislocations was observed in the seed region as in the GaN layer grown simply on sapphire substrate. Edge and mixed dislocations of around  $10^8 \text{ cm}^{-2}$  density were also observed in the coalescence region. Similar results were obtained by plan-view TEM observations.

The PL intensity profile of GaInN MQW on ELO-GaN is depicted in figure 9. The probe wavelength was 400 nm. The sample structure is illustrated at the bottom of the figure. As can be seen, the PL intensity profile of MQWs is similar to that of ELO-GaN. However, the difference in PL intensity between the wing and seed regions is much smaller than in the case of ELO-GaN in figure 7. Since the dislocation distribution in GaInN MQWs is believed to be the same as in GaN, the smaller intensity difference implies that the radiative efficiency of GaInN is not as sensitive to dislocation density as previously thought, due to carrier localization [46, 47].

Based on these results, we decided to fabricate a ridge stripe of LD on the wing region between the coalescence and seed regions.

#### 4.2. Improvement of cleaved facet

It is difficult to make a smoothly cleaved facet of an LD grown on a sapphire substrate because the *m*-surface (1-100) of GaN, which could be a weakly cleaved facet, is rotated  $60^\circ$  compared with that of the sapphire substrate. Of course, a smoothly cleaved facet can be obtained for an LD grown on a GaN substrate; however the threading-dislocation density of a GaN substrate is larger than that in the wing region of ELO-GaN except for high pressure grown bulk GaN [48, 49], which is at present too small to fabricate an LD on it. The cleaved facet of the LD



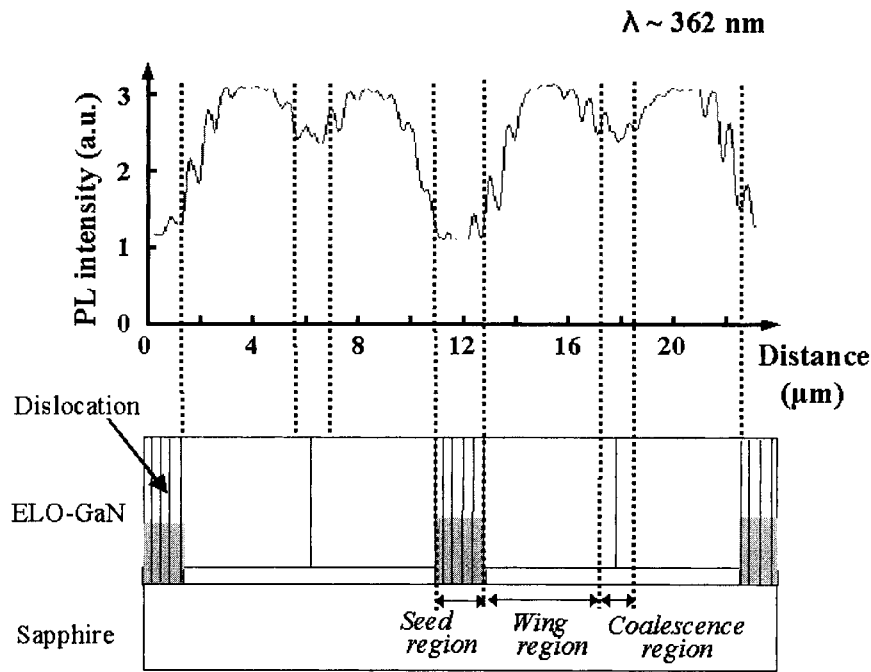


Figure 7. PL intensity line-profile for ELO-GaN [45].

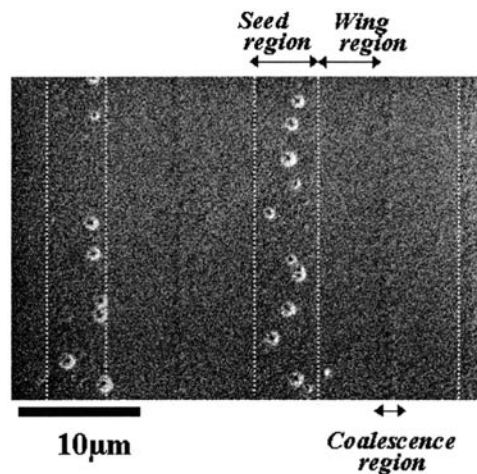


Figure 8. SEM image of an etched ELO-GaN surface.

on ELO-GaN is smoother than that on a sapphire substrate, as shown in figure 10, which shows surface profiles along the active layer measured by atomic force microscopy (AFM). The surface of the LD on sapphire, figure 10(a), is very rough. The roughness ( $R_a$ ) was more than 10 nm, which would cause mirror losses of at least 2–3%. On the other hand, there are flat areas in the LD on ELO-GaN, as can be seen in figure 10(b). In the seed region, the roughness is as high as that of the facet of LD on sapphire, while the surface of the wing region is as smooth as a GaAs cleaved surface ( $R_a < 1 \text{ nm}$ ). Consequently, we believe that ELO-GaN can

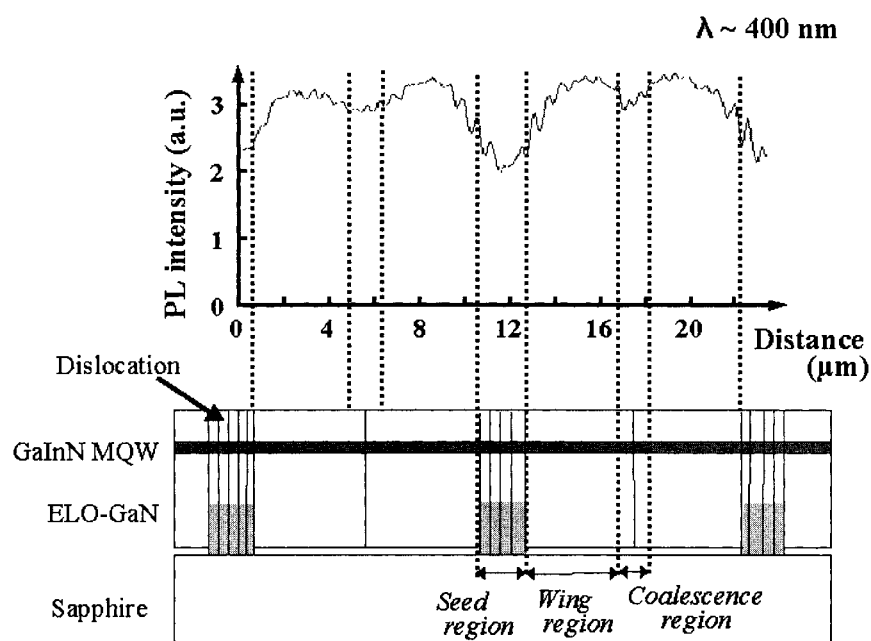
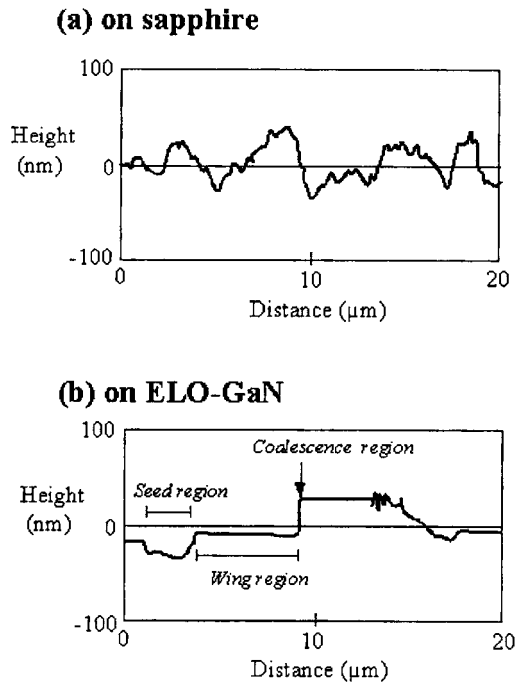


Figure 9. PL intensity line-profile for GaInN MQW grown on ELO-GaN [45].

be smoothly cleaved because GaN in the wing region is physically isolated from the sapphire substrate that does not cleave readily. This is another advantage of ELO-GaN as the underlying layer of the LD. It is notable that in the coalescence region there is a large step of about 30 nm. This is because the crystalline orientations of adjacent wing regions are not exactly the same.

### 5. Characteristics of high-power LDs on ELO-GaN

After obtaining a high-quality ELO-GaN with a low dislocation density and smooth cavity facets, we fabricated on it GaInN multiple quantum-well (MQW) LDs. A schematic cross-section of the LD is shown in figure 11. The underlying GaN layer, including ELO-GaN, was kept thinner than 5 μm because a thicker GaN layer on sapphire causes a serious problem of wafer bending [50]. An additional problem is that the stripe widths on the wafer varies and the lapping and cleaving process is more difficult with thicker layers. A 1.0 μm thick n-type Al<sub>0.08</sub>Ga<sub>0.92</sub>N cladding layer was grown over the ELO-GaN, followed by a 0.1 μm thick n-type GaN optical guiding layer, a Ga<sub>0.90</sub>In<sub>0.10</sub>N/Ga<sub>0.98</sub>In<sub>0.02</sub>N MQW active layer consisting of three pairs of a 3.5 nm thick Ga<sub>0.90</sub>In<sub>0.10</sub>N well layer and a 7.0 nm thick Ga<sub>0.98</sub>In<sub>0.02</sub>N barrier layer, a 20 nm thick p-type Al<sub>0.16</sub>Ga<sub>0.84</sub>N layer to minimize the electron overflow, a 0.1 μm thick p-type GaN optical guiding layer, a 0.5 μm thick modulation-doped p-type Al<sub>0.15</sub>Ga<sub>0.85</sub>N/GaN superlattice cladding layer consisting of 100 pairs of a 2.5 nm thick undoped Al<sub>0.15</sub>Ga<sub>0.85</sub>N layer and 2.5 nm thick Mg-doped GaN layer and a 0.1 μm thick p-type GaN contact layer. A 2.0 μm wide ridge stripe was formed on the wing region between the seed and coalescence regions. The remaining thickness of p-type layers outside the ridge was adjusted to 0.16 μm using RIE. Both sides of the ridge stripe were covered with SiO<sub>2</sub>. A p-type electrode consisting of Pd/Pt/Au was evaporated onto the p-type GaN contact layer. An n-type electrode of Ti/Pt/Au was evaporated on the underlying n-GaN after the n-GaN layer was exposed using RIE.



**Figure 10.** AFM surface profile of cleaved GaN grown on sapphire (a) and on ELO-GaN/sapphire (b) [45].

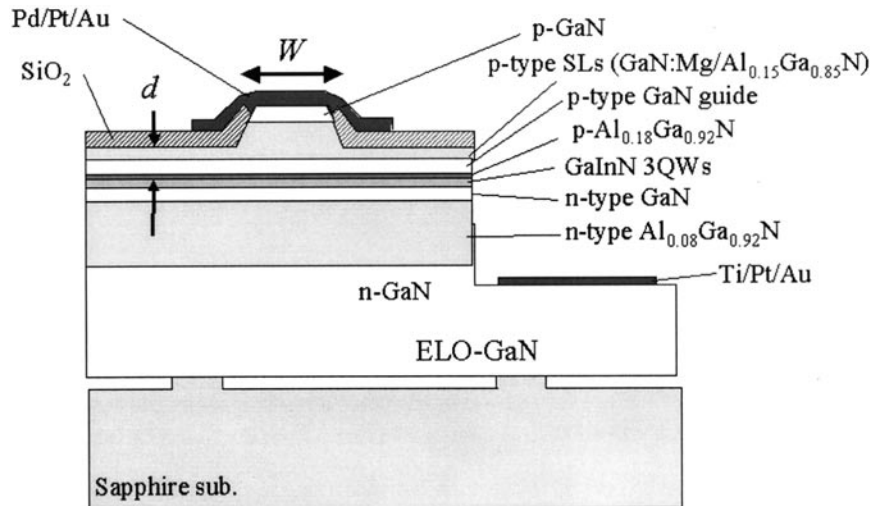


**Figure 11.** Schematic cross-section of a GaInN MQW LD grown on an ELO-GaN basal layer [45].

The wafer was lapped to a thickness of approximately  $100\ \mu\text{m}$  to easily cleave the facets. A  $600\ \mu\text{m}$  long cavity was formed in the  $\langle 1\text{-}100 \rangle$  direction of the GaN, which is parallel to the ELO stripe, using the conventional cleaving technique. The front facet was coated with an anti-reflection film of 10% reflectivity and the rear facet was coated with high-reflection film

of 95% reflectivity.

The characteristics of the LDs are dependent on the ridge stripe width ( $W$ ) and the residual etching depth next to the ridge stripe ( $d$ ). We optimized these parameters to  $2.0 \mu\text{m}$  for  $W$  and  $0.16 \mu\text{m}$  for  $d$ , in an attempt to minimize the consumption power at 30 mW, as reported previously [44, 45]. As shown in figure 12, the typical threshold current was 33 mA, which corresponds to a threshold current density ( $J_{th}$ ) of  $2.8 \text{ kA cm}^{-2}$ , and the voltage at the threshold ( $V_{th}$ ) was 4.8 V. The typical operating current ( $I_{op}$ ) and operating voltage ( $V_{op}$ ) for 30 mW cw operation were 59 mA and 5.4 V, respectively. There was no kink in the  $L-I$  curve below 50 mW under cw operation.

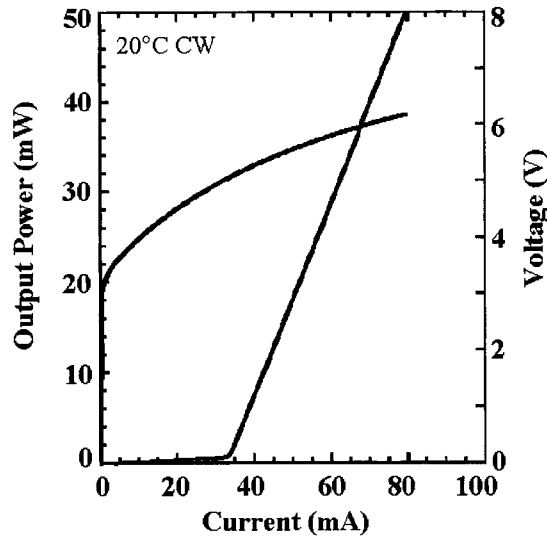


Figure 12. Typical  $L-I$  and  $I-V$  characteristics of GaN-based LD.

A comparison of the  $L-I$  characteristics of an LD on ELO-GaN to that on sapphire is shown in figure 13. The threshold currents of the LD on ELO-GaN and the LD on sapphire are 53.4 mA and 57.0 mA, respectively. The LD on ELO-GaN has a slope efficiency of  $1.21 \text{ W A}^{-1}$ , which is higher than the  $0.92 \text{ W A}^{-1}$  efficiency of the LD on sapphire. As a result, the operating current of the LD on ELO-GaN at 30 mW is roughly 10 mA lower than that of the LD on sapphire. These improvements in  $I_{op}$  and  $\eta$  are ascribed to the reduction of non-radiative centres and the smoother cleaved facet, which are advantages of ELO-GaN as previously ascribed.

The emission spectrum at 30 mW is shown in figure 14. Multi-mode emission was observed at a wavelength of around 404 nm. The peak separation was about 0.038 nm. The far-field patterns (FFP) are shown in figure 15. Full width at half maximum angles parallel and perpendicular to the junction plane were  $8^\circ$  and  $27^\circ$ , respectively, and hence the aspect ratio was around 3.4. These LDs exhibited a fundamental transverse mode up to 30 mW. The temperature dependence of  $L-I$  characteristics under cw conditions between  $20^\circ\text{C}$  and  $80^\circ\text{C}$  is shown in figure 16. High-power operation was realized up to  $80^\circ\text{C}$ . The characteristic temperature was estimated to be 132 K. The results of a lifetime test of an LD under  $60^\circ\text{C}$  cw conditions and at a constant output power of 30 mW are shown in figure 17. The LD was still functional after operating for more than 1000 h.

The lifetimes of LDs under 30 mW cw operation at  $25^\circ\text{C}$  are plotted against consumption power ( $I_{op} \times V_{op}$ ) in figure 18. Although the lifetime of these LDs tends to increase as

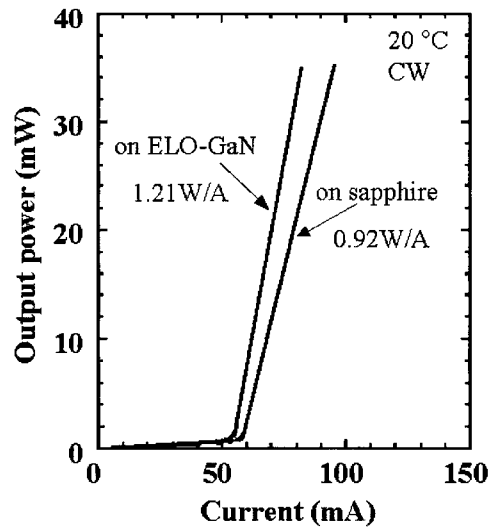


Figure 13. Comparison of  $L$ - $I$  characteristics for GaN-based LD grown on sapphire and ELO-GaN/sapphire [45].

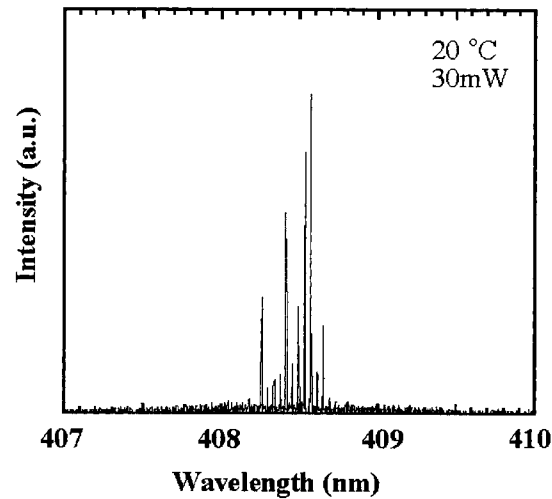


Figure 14. Laser emission spectrum measured under cw operation at output power of 30 mW [45].

consumption power decreases, the lifetime of LDs on ELO-GaN is an order of magnitude greater than that of LDs on sapphire substrates at low power consumption. This clearly demonstrates that the lifetime is closely related to not only dislocation density in an LD stripe but also the initial consumption power, and that ELO-GaN is very effective in reducing the dislocation density and yielding reliable LDs for practical use.

On the other hand, the long lifetime was obtained when threading-dislocation density in ELO-GaN was only reduced to  $10^6 \text{ cm}^{-2}$ , which is a relatively small reduction as compared with threading-dislocation density in GaAs- and InP-based LDs. We believe that the multiplication of non-radiative centres is very slow in GaN-based LDs, possible due to the innate character of the GaN-based semiconductor itself.

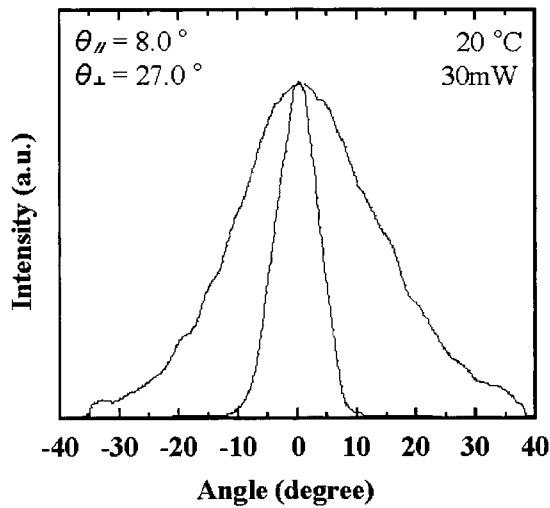


Figure 15. Far-field patterns measured under cw operation at output power of 30 mW [45].

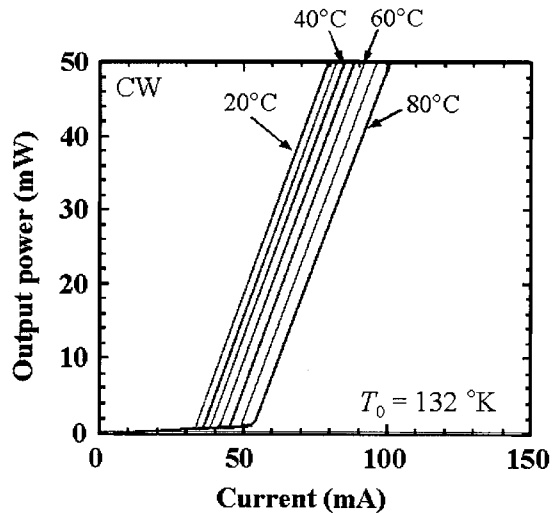


Figure 16. Temperature dependence of  $L$ - $I$  characteristics under cw operation [45].

## 6. Conclusion

The density of threading dislocations in GaN grown on sapphire substrate was first reduced to several times  $10^8 \text{ cm}^{-2}$  by the development of RP-MOCVD growth, then to  $10^6 \text{ cm}^{-2}$  by using the ELO growth technique. The characteristics of a GaN-based LD were drastically improved by fabricating the laser stripe just above the wing region of ELO-GaN. The cleaved facet then became smoother and this strongly contributed to the improvement of the LD's characteristics. The lifetime of the LD strongly depends not only on the threading dislocation density but also on the power consumption. We believe that the multiplication of the non-radiative centres around the threading dislocations is slow, because a long lifetime of over 1000 hours was demonstrated under  $60^\circ\text{C}$  cw condition at a constant output power of 30 mW although there

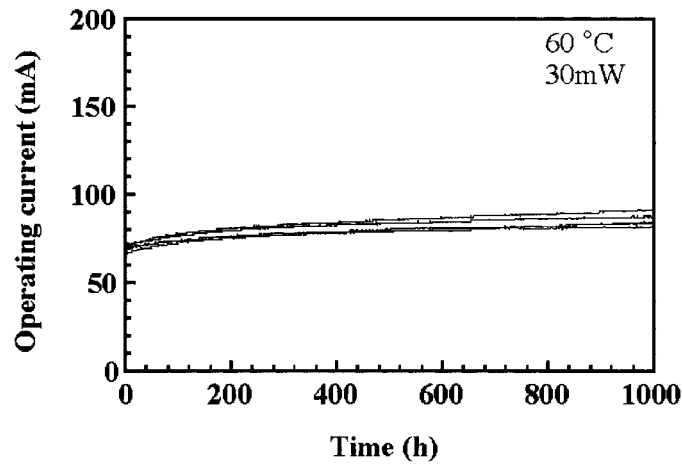


Figure 17. Lifetime test of the GaN-based LD under 60 °C cw operation at output power of 30 mW.

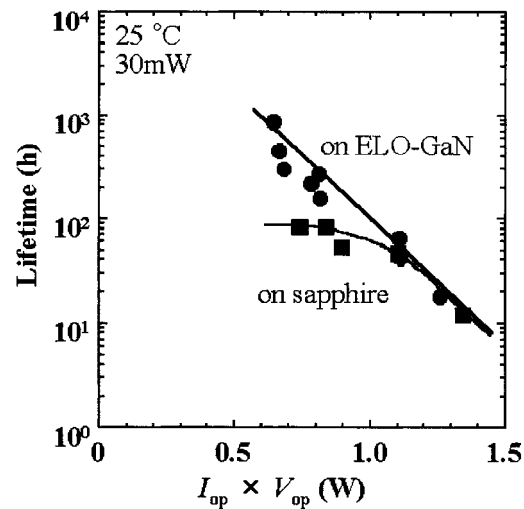


Figure 18. Dependence of lifetime on the initial consumption power ( $I_{op} \times V_{op}$ ) for GaN-based LD grown on sapphire and ELO-GaN/sapphire [45].

is still a threading-dislocation density of several times  $10^6 \text{ cm}^{-2}$  in the LD. Until a large GaN substrate with low threading-dislocation density is realized, GaN-based LDs grown on ELO will be used as a practical light source for high-density optical-storage systems.

### Acknowledgments

The authors would like to thank K Honda, K Tamamura and Dr O Kumagai for their encouragement during this work.

### References

- [1] Akasaki I, Amano H, Sota S, Sakai H, Tanaka T and Koike M 1995 *Japan. J. Appl. Phys.* **34** L1517

- [2] Nakamura S, Senoh M, Nagahama S, Iwasa N, Yamada T, Matsushita T, Kiyoku H and Sugimoto Y 1996 *Japan. J. Appl. Phys.* **35** L74
- [3] Nakamura S, Senoh M, Nagahama S, Iwasa N, Yamada T, Matsushita T, Sugimoto Y and Kiyoku H 1996 *Appl. Phys. Lett.* **69** 4056
- [4] Edmond J, Bulman G, Kong H S, Leonard M, Doverspike K, Weeks W, Nicum J, Sheppard S, Negley G and Slater D 1997 *Proc. 2nd Int. Conf. on Nitride Semiconductors* p 448
- [5] Kobayashi T, Nakamura F, Naganuna K, Tojyo T, Nakajima H, Asatsuma T, Kawai H and Ikeda M 1998 *Electron. Lett.* **34** 1494
- [6] Kuramata A, Kubota S, Soejima R, Domen K, Horino K and Tanahashi T 1998 *Japan. J. Appl. Phys.* **37** L1373
- [7] Kuramoto M, Sasaoka C, Hisanaga Y, Kimura A, Yamaguchi A, Sunakawa H, Kuroda N, Nido M, Usui A and Mizuta M 1999 *Japan. J. Appl. Phys.* **38** L184
- [8] Kneissl M, Bour D P, Van de Walle C G, Romano L T, Northrup J E, Wood R M, Teepe M, Schmade T and Johnson N M 1999 *Appl. Phys. Lett.* **75** 581
- [9] Tsujimura A *et al* 1999 *Phys. Status Solidi a* **176** 53
- [10] Koike M *et al* 2000 *Proc. Int. Workshop on Nitride Semiconductors (Nagoya, 2000) (IPAP Conf. Series 1)* p 886
- [11] Ito S *et al* 2000 *Proc. Int. Workshop on Nitride Semiconductors (Nagoya, 2000) (IPAP Conf. Series 1)* p 892
- [12] Park Y *et al* 2000 *Tech. Digest Int. Workshop on Nitride Semiconductors (Nagoya, 2000)* p 145
- [13] Miyachi M 2001 *Extended Abstracts 48th Spring Meeting, 2001, Japan. Soc. Appl. Phys. Relat. Soc. No 1*, p 368
- [14] Nagahama S *et al* 2000 *Japan. J. Appl. Phys.* **39** L647
- [15] Ikeda M and Uchida S 2001 *Proc. China–Japan Workshop on Nitride Semiconductor Materials and Devices (Shanghai, 2001)* p 100
- Funato K *et al* *MRS Internet J. Nitride Semicond. Res.* at press
- [16] Ichimura I, Maeda F, Osato K, Yamamoto K and Kasami Y 2000 *Japan. J. Appl. Phys.* **39** 937
- [17] Tieke B, Dekker M, Pfeffer N, van Woudenberg R, Zhou G-F and Ubbens I P D 2000 *Japan. J. Appl. Phys.* **39** 762
- [18] Amano H, Akasaki I, Hiramatsu K, Koide N and Sawaki N 1988 *Thin Solid Films* **163** 415
- [19] Nakamura S 1991 *Japan. J. Appl. Phys.* **30** 1705
- [20] Usui A, Sunakawa H, Sakai A and Yamaguchi A 1997 *Japan. J. Appl. Phys.* **36** L899
- [21] Nam O H, Bremser M D, Zheleva T and Davis R F 1997 *Appl. Phys. Lett.* **71** 2638
- [22] Amano H, Kito M, Hiramatsu K and Akasaki I 1989 *Japan. J. Appl. Phys.* **28** L2112
- [23] Nakamura S, Mukai T and Senoh M 1994 *Appl. Phys. Lett.* **64** 1687
- [24] Lester S D, Ponce F A, Craford M G and Steigerwald A 1995 *Appl. Phys. Lett.* **66** 1249
- [25] Miyajima T, Ozawa M, Asatsuma T, Kawai H and Ikeda M 1997 *Proc. 2nd Int. Conf. on Nitride Semiconductors, ICNS'97 (Tokushima, 1997)* p 82
- Miyajima T, Ozawa M, Asatsuma T, Kawai H and Ikeda M 1998 *J. Cryst. Growth* **189/190** 768
- [26] Nakamura S 1997 *Proc. 2nd Int. Conf. on Nitride Semiconductors, ICNS'97 (Tokushima, 1997)* p 444
- [27] Nishinaga T, Nakano T and Zhang S 1988 *Japan. J. Appl. Phys.* **27** L964
- [28] Asano T, Yanashima K, Asatsuma T, Hino T, Yamaguchi T, Tomiya S, Funato K, Kobayashi T and Ikeda M 1999 *Proc. 3rd Int. Conf. on Nitride Semiconductors, ICNS3 (Montpellier, 1999) We\_02*
- Asano T, Yanashima K, Asatsuma T, Hino T, Yamaguchi T, Tomiya S, Funato K, Kobayashi T and Ikeda M 1999 *Phys. Status Solidi a* **176** 23
- [29] Asatsuma T *et al* 2000 *10th Int. Conf. on Metal–Organic Vapor Phase Epitaxy (Sapporo, 2000)* Tu-P44
- Asatsuma T *et al* 2000 *J. Cryst. Growth* **221** 640
- [30] Miyajima T *et al* *Mater. Sci. Eng. B* **82** 248
- [31] Shiojima K 2000 *J. Vac. Sci. Technol. B* **18** 37
- [32] Hong S K, Yao T, Kim B J, Yoon S Y and Kim T I 2000 *Appl. Phys. Lett.* **77** 82
- [33] Hino T, Tomiya S, Miyajima T, Yanashima K, Hashimoto S and Ikeda M 2000 *Appl. Phys. Lett.* **76** 3421
- [34] Miyajima T, Hino T, Tomiya S, Yanashima K, Hashimoto S, Kobayashi T, Ikeda M, Satake E, Tokunaga E and Masumoto Y 2000 *Proc. Int. Workshop on Nitride Semiconductors (Nagoya, 2000) (IPAP Conf. Series 1)* p 536
- [35] Yanashima K *et al* 1999 *40th Electron. Mater. Conf. (VA, 1998)*
- Yanashima K *et al* 1999 *J. Electron. Mater.* **28** 287
- [36] Funato K, Hashimoto S, Yanashima K, Nakamura F and Ikeda M 1999 *Appl. Phys. Lett.* **75** 1137
- [37] Sakai A, Sunakawa H and Usui A 1998 *Appl. Phys. Lett.* **73** 481
- [38] Fini P, Zhao L, Moran B, Hansen M, Marchand H, Ibbetson J P, DenBaars S P, Mishra U K and Speck J S 1999 *Appl. Phys. Lett.* **75** 1706
- [39] Honda Y, Iyechika Y, Maeda T, Miyake H, Hiramatsu K, Sone H and Sawaki N 1999 *Appl. Phys. Lett.* **38** L1299
- [40] Tomiya S, Hino T, Kijima S, Asano T, Nakajima H, Funato K, Asatsuma T, Miyajima T, Kobayashi K and



- Ikeda M 2000 *Proc. Int. Workshop on Nitride Semiconductors (Nagoya, 2000) (IPAP Conf. Series 1)* p 284
- [41] Tomiya S, Funato K, Asatsuma T, Hino T, Kijima S, Asano T and Ikeda M 2000 *Appl. Phys. Lett.* **77** 636
- [42] Zheleva T S, Smith S A, Thomson D B, Gehrke T, Linthicum K J, Rajagopal P, Carlson E, Ashmawi W M and Davis R F 1999 *MRS Internet J. Nitride Semicond. Res.* **4S1** G3.38
- [43] Nakamura S, Senoh M, Nagahama S, Matsushita T, Kiyoku H, Sugimoto Y, Kozaki T, Umemoto H, Sano M and Mukai T 1999 *Japan. J. Appl. Phys.* **38** L226
- [44] Uchida S 2000 *Proc. SPIE* **3947** 156
- [45] Tojyo T 2000 *Proc. Int. Workshop on Nitride Semiconductors (Nagoya, 2000)* p 878
- [46] Narukawa Y, Kawakami Y, Funato M, Fujita S, Fujita S and Nakamura S 1997 *Appl. Phys. Lett.* **70** 981
- [47] Chichibu S, Wada K and Nakamura S 1997 *Appl. Phys. Lett.* **71** 2346
- [48] Porowski S 1999 *MRS Internet J. Nitride Semicond. Res.* **4S1** G1.3
- [49] Oda O, Inoue T, Seki Y, Wakahara A, Yoshida A, Kurau S, Yamada Y and Taguchi T 2000 *IEICE Trans. Electron.* **E83-C** 639
- [50] Takeya M *et al* 2000 *10th Int. Conf. on Metal–Organic Vapor Phase Epitaxy (Sapporo, 2000)* Fr-A7  
Takeya M *et al* 2000 *J. Cryst. Growth* **221** 646